

# Kinetic energy functionals and the $N$ -representability of the electron pair-density given by the classical map hyper-netted-chain (CHNC) method.

M.W.C. Dharma-wardana

National Research Council of Canada, Ottawa, Canada, K1A 0R6 \*

(Dated: December 21, 2024)

The classical-map hyper-netted-chain (CHNC) method for determining the pair-distribution function (PDF) of interacting electrons in a system of uniform density has been proposed as an accurate and fast method which uses the well known non-interacting quantum PDF as its initial input. It uses a kinetic energy functional in the form of a classical-fluid temperature. Here we address the question of the  $N$ -representability of the CHNC pair densities. Since a knowledge of the PDFs of a system are sufficient to obtain the static- and linear-transport properties of electron-ion systems, we review the use of the CHNC method for completely classical calculations of interacting multi-component electron-ion systems as a means of reproducing e-e, e-ion and ion-ion PDFs usually obtained via expensive quantum Monte Carlo methods or from density-functional molecular dynamics simulations. CHNC methods scale as the zeroth power of the number of particles in the system.

PACS numbers: 31.10.+z, 71.10.-w, 71.15.Nc

## INTRODUCTION

The wavefunction  $\Psi(\vec{r}_1, \dots, \vec{r}_N, \{\vec{R}_j\})$  of an  $N$ -electron quantum system depends on  $3N$  space coordinates, spin indices, as well as coordinates  $\{\vec{R}_j\}$  specifying the configuration of the nuclei present in the system. In the following at first we focus specifically on the electron subsystem and drop the references to the ions which are treated as passively providing an ‘external potential’ to the electrons. The ion subsystem is typically a system of classical particles, while the electrons are typically a quantum system. Then, in the final section we treat the two component system of interacting electrons and ions.

Our objective is to represent the interacting quantum electron subsystem at the extreme quantum limit of  $T = 0$  by an ‘equivalent’ interacting classical Coulomb fluid, at least in a statistical sense. That is to say, for example, that the pair distribution functions (PDFs) of the electron subsystem are reproduced in the classical Coulomb fluid. A formal requirement of such maps is the need to satisfy the  $N$ -representability constraints that all quantum densities are expected to satisfy [1, 2].

The many-electron wavefunction contains significantly more information than necessary for the calculation of energies and properties of physical systems. Furthermore, as  $N$  becomes large, the resolution of the many-particle Schrodinger or Dirac equation, or their quantum Monte Carlo (QMC) formulations becomes numerically prohibitive. A way out of this problem is presented by the Hohenberg-Kohn theorem basic to density functional theory (DFT), which asserts that the ground-state energy  $E$  of the system is a functional of just the *one-body* electron density  $n(r)$  [3–5].

$$n(r) = \int d\vec{r}_2 \dots d\vec{r}_N |\Psi(\vec{r}_1, \dots, \vec{r}_N)|^2, \quad (1)$$

The Hohenberg-Kohn theorem is a counter-intuitive re-

sult since the many-particle Hamiltonian

$$H = T + V(\vec{r}) + V_{ee}(\vec{r}_1, \vec{r}_2) \quad (2)$$

explicitly contains the electron-electron Coulomb potential – a two-body interaction. The many-body effects of this interaction, as well as corrections arising from the kinetic energy operator  $T$  acting on the many-body wavefunction  $\Psi$  are contained in a one-body energy functional known as the XC-functional of DFT, viz,  $E_{xc}([n])$ . Since the exchange energy component of the Hartree-Fock energy is explicitly known, it is sometimes convenient to define only the correlation energy  $E_c$ . However, it must be noted that grouping of  $E_x$  and  $E_c$  together is justified (especially for free-electron systems like metals and plasmas at finite- $T$ ) due to important cancellations between the two terms [6]

$$H\Psi = E\Psi, \quad E = E_{\text{HF}} + E_c. \quad (3)$$

Here  $E_{\text{HF}}$  is the mean-field energy which is the Hartree-Fock energy of the electron system. In effect, the relevant many-body information is contained in the XC-functional whose functional derivative with respect to the one-body density gives the Kohn-Sham one-body XC-potential. The question of the existence of such a potential leads to the *V-representability problem* which will not be discussed here, except for a brief remark prior to the conclusion.

The Hohenberg-Kohn theory posits that the exact ground state one-body density  $n(r)$  is precisely the one which minimizes the ground state energy. Its extension to finite- $T$  [7] states that the Helmholtz free energy  $F$  of the system is a functional of the one-body density, and that  $F$  is a minimum for the true density.

However, prior to the formulation of DFT, it was already recognized that the ground state energy can be expressed entirely in terms of the two-body density  $n(\vec{r}_1, \vec{r}_2)$ , although the possibility of a reduction to a

one-body functional was not suspected. The two-body density matrix is obtained by integrating all but two of the space and spin variables of the  $N$ -body density, viz., the square of the many-body wavefunction. This is also known as the two-particle reduced density matrix (2-RDM), and identified with the pair-distribution function (PDF) itself (depending on the prefactors used in various definitions). The pair-distribution function  $g(\vec{r}_1, \vec{r}_2)$  can be written as  $g(\vec{r})$  for a uniform system, and gives the probability of finding a second particle at the radial distance  $r$ , while the first particle is taken as the origin.

Furthermore, the one-body density in a system where the origin of coordinates is attached to one of the particles automatically becomes a 2-body density in the laboratory frame, and hence the PDF of homogeneous systems, e.g., a uniform Coulomb fluid, can be used to display the particle correlations. Hence, for a uniform fluid we have:

$$n(\vec{r}_1=0, \vec{r}_2=\vec{r}) = \bar{n} g_{12}(r).$$

While placing the origin on a particle is classically possible, more care is needed in the quantum problem of the uniform electron liquid (UEL) to be discussed below.

In 1955 Mayer proposed [8] to compute the ground-state energy of  $N$ -electron systems variationally as a functional of the two-electron reduced density matrix, i.e., the PDF, instead of the many-body wavefunction. Both  $\Psi$ , and the 2-RDM are unknown, but, unlike the wavefunction, the 2-RDM scales polynomially with the number  $N$  of electrons. However, the 2-electron density matrix must be constrained to represent a many-electron wavefunction for it to be a physically acceptable 2-density. Otherwise, the ground state energy for  $N > 2$  can even fall below the true ground state energy during a variational calculation. So the 2-electron density matrix must be constrained to represent an  $N$ -electron wavefunction. Coleman called these constraints  $N$ -representability conditions [1]. In the case of DFT, the Hohenberg-Kohn minimization must be carried out in a manner constrained to satisfy the requirements of  $N$ -representability [9, 10].

In effect, any theory of interacting electrons and their reduced densities that avoids the calculation of the  $N$ -electron wavefunction is faced with the problem of ensuring the  $N$ -representability of the calculated densities, PDFs etc. The implementation of DFT used in the original Kohn-Sham theory [4] maps the interacting electrons to a set of non-interacting electrons at the *interacting density*, and calculates the ‘Kohn-Sham’ one-electron wavefunctions  $\phi_j(r)$  using a local-density approximation (LDA) to the exchange-correlation potential. Hence the corresponding many-body wavefunction is a Slater determinant, and the Kohn-Sham theory gives rise to the  $N$ -representable density  $n(r)$  given by:

$$n(r) = \sum_j |\phi_j(r)|^2 f(\epsilon_j). \quad (4)$$

At  $T = 0$  the Fermi occupation factors  $f(\epsilon_j)$  reduce to unity for occupied states, and zero for unoccupied states. Hence the summation at  $T = 0$  is over occupied states, while at finite- $T$  such summations, and the required size of the basis sets become rapidly prohibitive as  $T$  increases. Here  $\epsilon_j$  are the Kohn-Sham eigenvalues of the non-interacting electron system corresponding to the KS eigenfunctions  $\phi_j(r)$ . So, the KS  $\phi_j(r), \epsilon_j$  have the physical meaning of being the eigenstates and eigenenergies of the fictitious non-interacting electron map of the interacting electron system, rather than those of the original interacting electron system. The Kohn-Sham procedure guarantees the  $N$ -representability of the density and treats the kinetic energy explicitly, without attempting to use a kinetic energy (K.E.) functional as in ‘orbital-free’ DFT theories.

The simplest ‘orbital free’ theory is the Thomas-Fermi theory, where the K.E. functional is taken to be the Thomas-Fermi kinetic energy at each local density. Various extensions of Thomas-Fermi theory in the form of orbital-free DFT, as well as applications of the method exist [5, 11–15]. Many of these formulations use the Weizsacker ansatz where just one orbital, viz.,  $\phi(r) = \sqrt{n(r)}$  is used in a Schrodinger-like equation to obtain the kinetic energy. However, these methods need further improvement as the non-local nature of the kinetic energy operator has proved to be a great stumbling block. The excellent review by Carter [11], littered with many acronyms, shows the highly heuristic nature of the search for a K.E. functional that has gone on for some four score years.

A kinetic energy functional is unnecessary for simple ‘one-center’ calculations typical in atomic physics or in methods that use the neutral-pseudo-atom (NPA) model [16–18, 21, 22] of electron-ion systems where the  $N$ -ion problem is replaced by a ‘one-ion’ problem. However, the simulations done with codes like the VASP [23] or ABINIT [24] use some 100-200 nuclear centers  $N_I$  and even up to  $N = N_e \sim 1000$  electrons in each step of a series of molecular-dynamics (MD) simulations. Hence such methods are extremely expensive and become prohibitive for many problems in warm-dense matter, materials science and biophysics.

Such quantum calculations can be greatly simplified as follows.

1. By the construction of an explicit electron kinetic energy functional in terms of the one-body electron density  $n(\vec{r})$ .
2. Using a neutral pseudo-atom (NPA) approach where the  $N_I$  nuclei are replaced by a one-body ion distribution  $\rho(\vec{r})$  [16, 17], while the electrons are described as usual by the distribution  $n(\vec{r})$ . Since ions are classical particles in most applications, we choose an ion as the origin of coordinates. Two coupled KS-equations for the two subsystems (ions

and electrons) arise from the functional differentiation of the free energy.

$$\frac{\delta F([n], [\rho])}{\delta [n]} = \mu_e, \quad \frac{\delta F([n], [\rho])}{\delta [\rho]} = \mu_I. \quad (5)$$

The electron and ion chemical potentials appear on the RHS. The first equation reduces to a one-center Kohn-Sham equation for the electrons in the field of the ion at the origin, while the second equation reduces to an HNC-like equation [16, 17]. If there are many types of ions, a coupled set of one-center equations appear [18].

This approach to interacting electron-ion systems does not invoke the Born-Oppenheimer (BO) approximation, but the use of BO can further simplify the implementation. The solution of such one-center equations is numerically extremely rapid, even at finite  $T$ . Such calculations reproduce the PDFs  $g_{cc}(r)$  of, say, molten carbon (or silicon) containing a complex bonding structure that are only exposed by lengthy and expensive DFT-MD simulations. That is, the *one-center* NPA calculations include sufficiently good ion-ion classical correlation functionals that they are able to reproduce the peak in the  $g_{cc}(r)$  that correspond to the 1.4-1.5Å C-C covalent bond as well the peaks in the  $g(r)$  due to the hard sphere-like packing effects seen in the DFT-MD simulations [21, 22].

3. The NPA approach can also be further simplified by the use of a K.E. functional; but the NPA calculation is already so rapid that nothing is gained on using approximations to the K.E. functional that bring in their own errors.

It should be noted that a number of similar one-center models use the name ‘‘Neutral Pseudo Atom’’, although there are some significant differences. Thus Chihara uses a neutral-pseudo-atom construction where he begins from the HNC equation and the identification of a ‘quantum’ Ornstein-Zernike equation applied to electron-ion systems [19]. While this is reasonable for the ion-ion, and perhaps even for the ion-electron system, it is not clear if it is at all valid for the electron-electron system. Thus Anta and Louis [20] in their implementation of an NPA using Chihara’s quantum HNC (qHNC) scheme are cautious enough to not to use the e-e qHNC equations proposed by Chihara. The NPA approach proposed by the present author and Perrot simply uses DFT for both electrons and ions, and invokes the HNC and bridge diagrams only to construct an ion-ion correlation functional [16, 18].

On the other hand, in the CHNC the electrons are replaced by a classical Coulomb fluid having the same PDFs as quantum electrons, and hence we only need to

use the classical OZ equation regarding which there is no controversy.

A simple test of the accuracy of theories that seek to present an explicit kinetic energy functional would be to apply them to the uniform electron gas in the presence of a test charge at the origin and compare the resulting charge densities with more exact calculations. The test charge should be a negative charge to simulate a conditional  $g_{ee}(r)$  calculation.

Several exact requirements on the K.E. functional (such as positivity) have been demonstrated, and their violation in various implementations has also been noted [25, 26]. On the other hand, as far as we are aware, there has been no attempt to examine what type of ‘orbital-free’ formulations lead to  $N$ -representable densities, or even whether they lead to non-negative electron-electron pair-distribution functions. Even without such tests, the available K. E. functionals are known to be far less accurate than KS calculations. Furthermore, such calculations may give energies that fall *below* the exact energies, as the approximate K.E. functionals may not satisfy the  $N$ -particle variational principle, since even some Kohn-Sham calculations that use generalized gradient approximations show such anomalies [27].

The study of the electron distribution in a uniform electron liquid (UEL) when a test electron is placed at the origin naturally leads to the question of the direct calculation of the physically valid  $g_{ee}(r)$  of the UEL rather than for a ‘test particle’. Here, not only must we overcome the problems involved in modeling the electron kinetic energy functional, but we must also avoid any *selection* of an electron on being held at the origin whereby it is made into a specific ‘test particle’ rather than an electron. A way around many such problems is opened up if a valid ‘classical representation’ of the quantum electrons can be carried out, at least in a statistical sense [28].

In the following we review the classical-map hyper-netted-chain (CHNC) scheme that has been used successfully [28–31] for a number of uniform systems (3D and 2D UELs, electron-proton plasmas [34], thick electron layers, double quantum wells [35]) etc. We examine if the pair-densities obtained via the classical-map technique are  $N$ -representable.

### CLASSICAL-MAP HYPER-NETTED-CHAIN SCHEME.

Let us consider an  $N$  electron system in a volume  $V$  such that  $N/V = \bar{n}$ , forming a uniform electron liquid in the presence of a neutralizing positive background. The electron eigenfunctions for the self-consistent mean-field problem (Hartree as well as Hartree-Fock models) are simple plane waves  $\phi_j(r) = \phi_{\vec{k}\sigma}(\vec{r}) = (\bar{n}/N)^{1/2} \exp(i\vec{k} \cdot \vec{r}) \zeta_\sigma$ . Here  $j$  is an index carrying any relevant quantum numbers including the spin index  $\sigma$  associated with the

spin function  $\zeta$ . Here  $\sigma = 1, 2$  or ‘up, down’, specifies the two possible spin states. Some of the vector notation will be suppressed for simplicity as we are dealing with a uniform liquid which has spherical symmetry in 3D and planar symmetry in 2D. The spin index may also be suppressed where convenient.

### The non-interacting pair-distribution function $g^0(r)$

The many-electron wavefunction for non-interacting electrons, as well as for Hartree-Fock (mean-field) electrons may be written as the normalized antisymmetric product of plane waves [36], i.e, a Slater determinant  $D(\phi_1, \dots, \phi_j)$  of  $N$ -plane waves. Its square is the  $N$ -particle density matrix, while the pair-distribution function is the two particle density matrix [37]. The latter is obtained by integrating over all but two space coordinates and summing over the  $N - 2$  spin variables. At finite temperatures, the  $N$ -electron problem actually needs a very large number  $\mathcal{N} > N$  of plane waves as electron occupations in quantum states become a thermal distribution given by the Fermi function appropriate to the given temperature. At  $T = 0$  all occupation numbers reduce to unity or zero, and we can use a plane-wave basis set of  $N$  functions.

$$g_{\sigma_1, \sigma_2}(\vec{r}_1, \vec{r}_2) = V^2 \sum_{\sigma_3 \dots \sigma_N} \int d\vec{r}_3 \dots \vec{r}_N D(\phi_1, \dots, \phi_j). \quad (6)$$

If the spins are anti-parallel, then the non-interacting PDF,  $g_{\sigma, \sigma'}^0(r)$  is unity for all  $\vec{r}$  as the presence of a particle at  $\vec{r}_1$  has no effect on the particle of opposite spin at  $\vec{r}_2$ . Denoting  $(\vec{r}_1 - \vec{r}_2)$  by  $\vec{r}$ , and  $(\vec{k}_1 - \vec{k}_2)$  by  $\vec{k}$ , it is easy to show that in the case of parallel spins,

$$g_{\sigma, \sigma}^0(\vec{r}) = \frac{2}{N^2} \sum_{\vec{k}_1, \vec{k}_2} f(k_1) f(k_2) \left[ 1 - \exp(i\vec{k} \cdot \vec{r}) \right] \quad (7)$$

$$f(k) = \left[ 1 + \exp\{(k^2/2 - \mu^0)/T\} \right]^{-1}. \quad (8)$$

Here we have generalized the result to finite  $T$ , where the temperature is measured in energy units. Given these results, the non-interacting PDFs, i.e.,  $g^0(r)$  are explicitly available at  $T = 0$ , and numerically at finite  $T$ .

$$g_{\sigma, \sigma}^0(r) = 1 - F^2(r) \quad (9)$$

$$F(r) = (6\pi^2/k_F^3) \int f(k) \frac{\sin(kr)}{r} \frac{kdk}{2\pi^2} \quad (10)$$

$$3D, \text{ zero } T, = 3 \frac{\sin(x) - x \cos(x)}{x^3}, \quad x = k_F r. \quad (11)$$

The equations contain the Fermi momentum  $k_F$  which is defined in terms of the mean density  $\bar{n}$  and the corresponding electron Wigner-Seitz radius  $r_s$ .

$$k_F = 1/(\alpha r_s), \quad r_s = [3/(4\pi\bar{n})]^{1/3}, \quad \alpha = (4/9\pi)^{1/3}. \quad (12)$$

Here we have assumed equal amounts of up and down spins (paramagnetic case) and defined  $k_F$ , the Fermi

wave vector. Similar expressions can be easily developed for the 2D electron layer [29], two coupled 2D-layers [35] and a two-valley 2D layer [38] which are multi-component cases of technological interest, e.g., in the study of metal-oxide field-effect transistors. The method has also been used successfully to obtain the local-field factors of 2D layers at zero and finite- $T$  [39], and for the study of thick 2D layers which are of technological interest [40].

### The $N$ -representability of $g^0(r)$ and its classical map

The PDFs  $g_{\sigma, \sigma'}^0(r) = 1 - \delta_{\sigma, \sigma'} F(r)$  calculated in the previous section were derived from the Slater determinant  $D(\phi_1 \dots, \phi_N)$  and hence manifestly  $N$ -representable. At this stage, irrespective of where it came from, we regard  $g^0(r)$  as a classical pair-distribution function for particles interacting by a classical pair potential  $\beta\mathcal{P}(r)$  where  $\beta$  is the inverse temperature. This is the first step in our classical map, and we may now identify one of the classical particles as being at the origin, without loss of generality, in a classical picture of the PDF. Clearly, for anti-parallel spins, i.e.,  $\sigma \neq \sigma'$ , the pair-potential  $\beta\mathcal{P}(r)$  is zero, while it is finite and creates the well-known ‘exclusion hole’ in the PDF of two parallel-spin fermions. Hence  $\mathcal{P}(r)$  has been called the ‘Pauli exclusion potential’ and should not be confused with the Pauli kinetic potential that appears in the theory of the kinetic energy functional.

F. Lado was the first to present an extraction of  $\beta\mathcal{P}(r)$  for 3D electrons at  $T = 0$  using the hyper-netted-chain (HNC) equation and the Ornstein-Zernike (OZ) equation [41] used in the theory of classical fluids. Note that only the dimensionless potential,  $\beta\mathcal{P}(r)$  is determined from the equations. Although the physical temperature  $T$  of the quantum fluid is zero, the temperature of the classical fluid invoked by the map is left undetermined in the ‘non-interacting’ system. The Pauli exclusion potential for 2D electrons was derived in Ref. [29]. Although the quantum electrons are not interacting via a Coulomb potential, they have the capacity to become entangled, and  $\beta\mathcal{P}(r)$  becomes a classical manifestation of entanglement interactions which scale as  $r/r_s$ , and hence extend to arbitrarily large distances [42]. Assuming that  $g^0(r)$  can be expressed as an HNC equation, we have:

$$g^0(r) = \exp[-\beta\mathcal{P}r + h^0(r) - c^0(r)] \quad (13)$$

$$h^0(r) = c^0(r) + \bar{n} \int d\vec{r}' h^0(|\vec{r} - \vec{r}'|) c^0(\vec{r}') \quad (14)$$

$$h^0(r) = g^0(r) - 1. \quad (15)$$

The first of these is the HNC equation, while the second equation is the O-Z relation. These contain the direct correlation function  $c^0(r)$  and the total correlation function  $h^0(r)$ . It should be noted that we have ignored the two-component character of the electron fluid (two spin

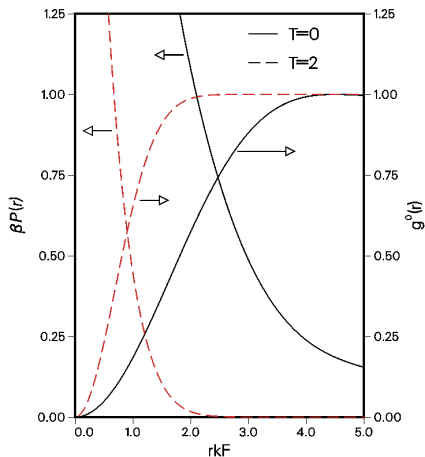


FIG. 1. The exclusion potential, Eq. 16, and the noninteracting PDF,  $g_{\sigma,\sigma}^0$  at  $T/E_F = 0$  (solid line) and at  $T/E_F = 2$  (dashed line). They are universal functions of  $r/r_s$ . The PDF  $g_{\sigma\neq\sigma'}^0(r) = 1$  as there is no exclusion effect for  $\sigma \neq \sigma'$ .

types) in the equations for simplicity, but the full expressions are given in, say, Ref. [28]. These equations can be solved by taking their Fourier transforms, and the Pauli exclusion potential can be obtained by the inversion of the HNC equation. The “Pauli exclusion potential”  $\mathcal{P}(r)$  is given by

$$\beta\mathcal{P}(r) = -\log[g^0(r)] + h^0(r) - c^0(r). \quad (16)$$

The Pauli exclusion potential is a universal function of  $rk_F$  or  $r/r_s$ . It is long ranged and mimics the exclusion effects of Fermi statistics. At finite  $T$  its range is about a thermal wavelength and is increasingly hard-sphere-like. The Fourier transform  $\beta\mathcal{P}(q)$  in 3D behaves as  $\sim 1/q$  for small  $q$ , and as  $\sim c_1/q^2 + c_2/d^4$  for large  $q$ .

Plots of  $\beta\mathcal{P}(r)$  and  $g^0(r)$  are given in Fig. 1.

### THE INTERACTING SYSTEM AND ITS CLASSICAL MAP

In the previous section we presented a classical fluid whose  $g^0(r)$  exactly recovers the PDFs of the noninteracting quantum UEL at any density, spin polarization or temperature. From now on, for simplicity we consider a paramagnetic electron gas (equal amounts of up spins and down spins) when writing equations which are treating a classical liquid, although spin-dependent quantities will be indicated where needed for clarity. Although the quantum liquid was ‘noninteracting’, the classical map already contains the pair potential  $\beta U_{ij} = \beta\mathcal{P}(r)$ .

On addition of a Coulomb interaction  $\beta V_{ij}(r)$  the total pair potential becomes

$$\beta U_{ij}(r) = \beta\mathcal{P}(r) + \beta V_{cou}(r). \quad (17)$$

The temperature  $T = 1/\beta$  occurring in Eq. 17 is as yet unspecified. In quantum systems the Coulomb interaction is given by the operator  $1/|\vec{r}_1 - \vec{r}_2|$  which acts on the eigenstates of the interacting pair. It can be shown (e.g., by solving the relevant quantum scattering equation) that the effective classical form of the Coulomb interaction,  $V_{cou}(r)$ ,  $r = |\vec{r}_1 - \vec{r}_2|$  acquires a diffraction correction for close approach. Depending on the temperature  $T$ , an electron is localized to within a thermal de Broglie wavelength. Thus, following earlier work on diffraction corrected potentials, (e.g., in Compton scattering in high-energy physics), or in plasma physics as in, e.g., Minoo et al.,[43] we use a “diffraction corrected” form:

$$V_{cou}(r) = (1/r)[1 - e^{-r/\lambda_{th}}]; \quad \lambda_{th} = (2\pi\bar{m}T_c f)^{-1/2}. \quad (18)$$

Here  $\bar{m}$  is the reduced mass of the interacting electron pair, i.e,  $m^*(r_s)/2$  a.u., where  $m^*(r_s)$  is the electron effective mass. It is weakly  $r_s$  dependent, e.g,  $\sim 0.96$  for  $r_s = 1$ . In this work we take  $m^*=1$ . The “diffraction correction” ensures the correct quantum behaviour of the interacting  $g_{12}(r \rightarrow 0)$  for all  $r_s$ . The essential features of the classical map are

1. The use of the exact non-interacting quantum PDFs  $g_{\sigma,\sigma'}^0(r)$  as inputs.
2. The use of a diffraction corrected Coulomb interaction.
3. The specification of the temperature of the classical Coulomb fluid  $T_{cf} = 1/\beta$  as the one that recovers the quantum correlation energy  $E_c(r_s)$ .

The selection of the classical fluid temperature is a crucial step. This is guided by the Hohenberg-Kohn-Mermin property that the exact minimum free energy is determined by the true one-body electron density  $n(r)$ . Since we are dealing with a uniform system, the Hartree energy  $E_H$  is zero. The exchange energy  $E_x$  is already correctly accounted for by the construction of the classical-map  $g^0(r)$  to be identical with the quantum  $g^0(r)$  at any  $T$  or spin polarization. Hence we choose to select the temperature  $T_{cf}$  of the classical Coulomb fluid to match the known DFT correlation energy  $E_c$  at each  $r_s$  at  $T = 0$ . Since this is most accurately known for the spin-polarized electron liquid,  $T_{cf}$  is determined from  $E_c(r_s)$  for full spin polarization. We select a trial temperature and solve for the interacting  $g(r, \lambda)$  for various values of the coupling constant  $\lambda$  in the interaction  $\lambda V_c(r)$  to calculate a trial  $E_c$  at the given  $r_s$  from the coupling constant integration. The temperature is iteratively adjusted until the

$E_c(r_s, T_{cf})$  obtained from the classical fluid  $g(r)$  agrees with the known quantum  $E_c(r_s, T = 0)$ . Given a quantum electron fluid at  $T = 0$ , the temperature of the classical fluid that has the same  $E_c$  is called its *quantum temperature*  $T_q$ . This was parametrized as:

$$T_q/E_F = 1.0/(a + b\sqrt{r_s} + cr_s) \quad (19)$$

for the range  $r_s = 1$  to 10, when  $T_q/E_F$  goes from 0.768 to 1.198. The values of the parameters  $a, b, c$  are given in Ref. [28].

There is no *a priori* reason to expect the  $\bar{n}g(r)$  obtained by this procedure to agree with the quantum  $n(r)$  except for the Hohenberg-Kohn theorem that requires  $n(r)$  to be the true density distribution when the energy inclusive of the XC-energy is correctly recovered. We have in fact no simple reason to expect that this classically obtained  $g(r)$  would correspond to an  $N$ -representable distribution, or that it would agree with the quantum Monte Carlo (QMC)  $g(r)$  at arbitrary  $r_s$ , and in particular, at high values of  $r_s$  when the Coulomb potential dominates the kinetic energy term in the Hamiltonian. Many well-known quantum procedures (e.g., that of Singwi et al. [46, 47]) for the PDFs lead to negative  $g(r)$  as  $r_s$  is increased beyond unity.

However, as shown in Refs. [28, 29, 48] and subsequent work, the classical map HNC  $g(r)$  provides an accurate approximation to the QMC PDFs where available. Correlations are stronger in reduced dimensions. The 2D classical map was constructed using the modified-HNC equation where a hard-sphere bridge function was used, with the hard-sphere radius determined by the Gibbs-Bogoliubov criterion, as prescribed by Lado, Foils and Ashcroft [49]. Other workers [30, 31, 33] have examined different parametrization than our fit form Eq. 19. Sandipan and Dufty [32] examined the connection between the classical map approach and the method of quantum statistical potentials [44, 45]. They also proposed using additional conditions (besides the requirement that  $E_c$  is reproduced by  $T_{cf}$ ) to constrain the classical map.

Although  $E_c$  at  $T = 0$  were available when the classical map for the UEL was constructed, no reliable XC-functionals (beyond RPA) were available for the finite- $T$  electron liquid. Hence we proposed the use of the equation

$$T_{cf} = (T_q^2 + T^2)^{1/2} \quad (20)$$

as a suitable map for the finite- $T$  UEL. This was based on a consideration of the behaviour of the heat capacity and other thermodynamic properties of the UEL. Furthermore, using Eq. 20 it became possible to predict the XC-free energy  $F_{xc}(r_s, T)$  as well as the finite- $T$  PDFs of the UEL at arbitrary temperatures and spin polarizations. These were found to agree closely with the  $F_{xc}$  and PDFs reported 13 years later by Brown et al. [50] where they used Feynman Path-Integral Monte Carlo (PIMC)

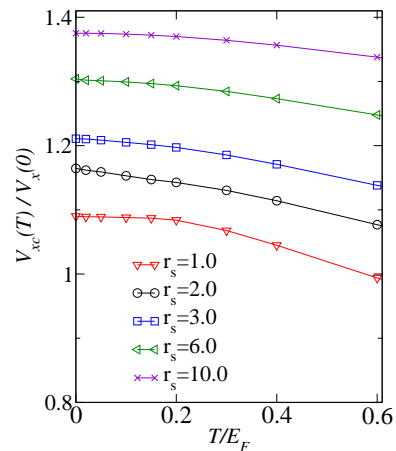


FIG. 2. (Color online) Finite- $T$  exchange and correlation free energy  $f_{xc}(r_s, T)$  per electron (Hartrees) versus the reduced temperature  $T/E_F$  in units of the Fermi energy. The symbols, are the path-integral Monte Carlo (PIMC) data of Brown et al. Ref. [50] as given in Ref. [51]. The continuous lines are from the classical-map HNC procedure of Perrot and Dharmawardana, Ref. [48]. The temperature range  $T/E_F < 1$  is the region of interest for WDM studies. The thermal-XC corrections to the  $T = 0$  XC-functional are most important near  $T/E_F \simeq 0.5$  and then decrease with increasing  $T$ .

simulations. The PIMC data have been parametrized by Karasiev et al, Ref. [51]. Calculations of  $F_{xc}$  using the finite  $T$  parametrization given by Perrot and Dharmawardana [48] are compared with the Feynman path results in Fig. 2. It should be noted that the parametrization of the finite- $T$  XC free energy given by Perrot et al. [48] explicitly incorporates the high- $T$  Debye-Hückel limit of  $F_c$  as well as the high- $T$  behavior of  $F_x(T)$ .

#### **$N$ -representability of the interacting $g(r)$ of the classical map.**

We note that the conditions  $n(r) = \bar{n}g(r) > 0$ , and  $\int n(\vec{r})d\vec{r} = N$  are always satisfied by the classical map procedure. Furthermore, the classical map becomes increasingly exact as  $T/E_F$  is increased and electrons become increasingly classical.

We present two arguments that lead us to conclude that the  $g(r)$  of the interacting UEL obtained by the classical map procedure is  $N$ -representable.

(1)**Argument based on the HNC equation being an  $N$ -representability conserving transformation.** Once the  $g^0(r)$  of the quantum fluid is evaluated we consider a classical fluid which has the same  $g^0(r)$ . The non-interacting  $g^0(r)$  and the corresponding  $n^0(r) = \bar{n}g^0(r)$  of the classical fluid are generated from the homogeneous density  $\bar{n}$  by a transformation where the origin of coordinates is moved to one of the particles. The corresponding

transformation of the density profile as written as:

$$n^0(r) = \mathcal{T}_0(r)\bar{n} \quad (21)$$

$$\mathcal{T}_0(r) = \exp[\beta\mathcal{P}(r) + h^0(r) + c^0(r)]. \quad (22)$$

$$(23)$$

The so generated  $n^0(r)$  is  $N$ -representable by its construction from a Slater determinant. Then, in a next step the interacting  $g(r)$  is generated from the  $N$ -representable non-interacting  $g^0(r)$  by a transformation which can be written as:

$$g(r) = \mathcal{T}_1(r)g^0(r) \quad (24)$$

$$\begin{aligned} \mathcal{T}_1(r) &= e^{[\beta V_{cou}(r) + \{h(r) - h^0(r)\} + \{c(r) - c^0(r)\}]} \\ &= \exp[\beta\{V_{cou}(r) + V_{pmf}(r)\}]. \end{aligned} \quad (25)$$

In effect, the uniform density  $\bar{n}$  has been transformed (by a selection of the origin of coordinates, and by switching on the Coulomb interaction) by a single composite transformation  $\mathcal{T} = \mathcal{T}_1\mathcal{T}_0$  with its components acting one after the other.

In equation 25 we have  $V_{pmf}(r)$  to indicate the correlation correction to the potential of mean force, expected to be a well-behaved function. The diffraction corrected classical Coulomb potential  $V_{cou}(r)$  has a finite-value at  $r = 0$ , and not singular, unlike the point-Coulomb potential  $1/r$ . Hence we may regard the above transformation as being mathematically equivalent to a type of smooth coordinate transformation of  $\vec{r}$  to another variable  $\vec{s}$

$$d\vec{s} = \mathcal{T}(r)\bar{n}d\vec{r} = n(r)d\vec{r}. \quad (26)$$

That is, the initial planewave states  $(\bar{n}/N)^{1/2} \exp(i\vec{k} \cdot \vec{r})$  are transformed to a new set  $(n(\vec{r})/N)^{1/2} \exp(i\vec{q} \cdot \vec{s}(r))$ . It is easily shown that they form a mutually orthogonal complete set. For instance, consider the initial planewave state used in the Slater determinant, i.e.,  $\phi_j(\vec{r}) = \phi_k(\vec{r})$  and consider its transformed state  $\tilde{\phi}_k(\vec{r})$  given below:

$$\phi_k(\vec{r}) = (\bar{n}/N)^{1/2} \exp(i\vec{k} \cdot \vec{r}) \quad (27)$$

$$\tilde{\phi}_k(\vec{r}) = (n(\vec{r})/N)^{1/2} \exp(i\vec{k} \cdot \vec{s}(\vec{r})). \quad (28)$$

We regard  $\vec{k}$  as an arbitrary  $k$ -vector and hence it is sufficient to transform  $\vec{r}$ , while the theory can also be constructed entirely in  $k$ -space in an analogous manner. The transformed wavefunctions  $\tilde{\phi}_k(\vec{r})$  have the following properties:

$$\int \tilde{\phi}_{k'}^*(\vec{r})\tilde{\phi}_k(\vec{r})d\vec{r} = \int \frac{n(\vec{r})}{N} e^{i(\vec{k}' - \vec{k}) \cdot \vec{r}} d\vec{r} \quad (29)$$

$$= \frac{1}{N} \int \exp\{i(\vec{k}' - \vec{k}) \cdot \vec{s}\} \frac{d\vec{s}}{N} \quad (30)$$

$$= \frac{(2\pi)^3}{N} \delta^3(\vec{k}' - \vec{k}). \quad (31)$$

Furthermore,

$$\int \tilde{\phi}_k^*(\vec{r})\tilde{\phi}_k(\vec{r}') \frac{d\vec{k}}{(2\pi)^3} = \frac{\delta^3(\vec{r} - \vec{r}')}{N}. \quad (32)$$

Hence the transformed functions  $\tilde{\phi}_k(\vec{r})$  form a complete orthogonal set. This implies that the initial Slater determinant  $D(\phi_{k_1}, \dots, \phi_{k_N})$  of the noninteracting electron system transforms to the determinant  $D(\tilde{\phi}_{k_1}, \dots, \tilde{\phi}_{k_N})$  of the interacting system, explicitly showing the  $N$ -representability of the  $n(r) = \bar{n}g(r)$  obtained via the classical map which consists of the application of the two transformations  $\mathcal{T}_1\mathcal{T}_0$ . Furthermore, the transformations commute, in the sense that one may first apply *only* the diffraction corrected Coulomb potential to non-interacting fermions to generate a  $g^c(r)$  for a Coulomb fluid, and then apply the Pauli exclusion potential to generate the fully interacting classical map inclusive of exchange-correlation effects, or *vice versa*. This is equivalent to iterating the HNC equations from the non-interacting state via two different paths, and indeed the two different procedures,  $\mathcal{T}_1\mathcal{T}_0$  and  $\mathcal{T}_0\mathcal{T}_1$  lead to the same final  $g(r)$ .

The above analysis confirms the  $N$ -representability of the pair-densities of the interacting uniform electron liquid generated by the classical map presented here.

## (2) Argument based on the $N$ -representability of the QMC density.

The diffusion quantum Monte Carlo (DQMC) calculations use a Slater determinant together with Jastro factors, and hence the DQMC procedure is based on an explicit many-body wavefunction whose variation produces a minimum energy and a corresponding  $E_c(r_s)$ . Hence its two-particle reduced density matrix, i.e., the electron-electron PDF is  $N$ -representable; the correlation energy  $E_c$  associated with the  $N$ -representable two-body density is the correlation contribution to the best approximation to the energy minimum as per Hohenberg-Kohn theorem, since the minimum is achieved only for the true density. The CHNC electron-electron PDFs agrees with the DQMC- $g(r)$  with *no attempt at fitting* the PDFs. The only input is the one number  $E_c(r_s)$  at each density introduced via the classical temperature  $T_{cf}$  - a classical kinetic energy. Thus, both the electron density  $\bar{n}g(r)$  and its  $E_{xc}$  agree with those of the  $N$ -representable density  $\bar{n}g_{DQMC}(r)$  as well as the energy  $E_{xc}$  from DQMC. Hence we conclude that the CHNC  $n(r)$  is at least as  $N$ -representable as the DQMC procedure.

It should be noted that the classical pair potential  $U(r) = \mathcal{P}(r) + V_{cou}(r)$  may be used in a classical molecular dynamics simulation to generate the interacting  $g(r)$  instead of using the HNC equations. It is also possible to generate the dynamics of such a fluid, e.g., determine  $S(k, \omega)$  by a classical simulation. However, the Pauli exclusion interaction is really a kinematic quantum effect and not a true 'interaction'. It is not known at present whether such a classical map  $S(k, \omega)$  agrees in detail with the quantum  $S(k, \omega)$  for an interacting electron fluid.

## CHNC METHOD FOR SYSTEMS OF INTERACTING ELECTRONS AND IONS

So for we have treated a system of electrons interacting with each other in the presence of a passive neutralizing background at arbitrary densities, spin polarizations and temperature, as defined in the UEL. We have discussed how the electrons can be replaced by an equivalent classical fluid in the sense that the interacting e-e PDF  $g_{ee}(r)$  can be computed accurately via classical statistical mechanics, giving us the one-body electron density  $n(r) = \bar{n}g_{ee}(r)$ . There is in fact no need to limit the ion density  $\rho(r)$  to the jellium limit used in the UEL. Instead we can return to the two density functional equations of the NPA, viz., Eqs. 5. As shown in the appendix to Ref. [16] these equations for  $n(r), \rho(r)$ , when applied to classical particles reduce to classical Kohn-Sham equations which are Boltzmann like distributions. In the classical case they can be reduced to two coupled HNC-like equations for the electrons and ions. The HNC equation (with or without a Bridge term) for the electrons replaced by their classical map is the CHNC equation that we have already discussed, except that the potential of mean force for the electron-ion case now contains an electron-ion interaction potential as well.

As an example, we take a system of ions of mean charge  $\bar{Z}$  with a mean density  $\bar{\rho}$  interacting with a neutralizing system of electrons at a mean density  $\bar{n} = \bar{Z}\bar{\rho}$ . For simplicity we assume that there is just one kind of ion, and that  $\bar{Z} = 1$  as for a hydrogenic system. We denote the ion species by  $A^+$ . The coupled CHNC-MHNC equations are given in Refs. [34, 52] and discussed below.

The densities  $\bar{\rho}$  and  $\bar{n}$  are equal since the ion charge  $\bar{Z} = 1$ . Consider a fluid of total density  $n_{tot}$ , with three species. Let  $x_i = n_i/n_{tot}$ ,  $n_{tot} = \bar{\rho} + \bar{n}$ . The physical temperature is  $T$ , while the inverse temperature of the electrons is  $1/\beta_{ee}$ , with  $1/\beta_{ee} = \sqrt{T^2 + T_q^2}$ . For the ion  $A^+$ , no quantum correction is needed and  $T_{AA} = 1/\beta_{AA}$  is  $T$ . So the electron-ion system in CHNC is a two-temperature system. The coupled CHNC equations require a  $\beta_{eA}$  and how this is treated will be discussed below. So, using  $T_{ij} = 1/\beta_{ij}$  and  $\phi_{ij}$  for the interparticle temperatures and pair-potentials, the coupled classical equations for the PDFs and the Ornstein-Zernike relations are:

$$g_{ij}(r) = e^{[-\beta_{ij}\phi_{ij}(r) + h_{ij}(r) - c_{ij}(r) + B_{ij}(r)]} \quad (33)$$

$$h_{ij}(r) = c_{ij}(r) + \sum_s n_s \int d\mathbf{r}' h_{i,s}(|\mathbf{r} - \mathbf{r}'|) c_{s,j}(\mathbf{r}') \quad (34)$$

The pair potential  $\phi_{ij}(r)$  between e-e is just the Coulomb potential  $V_{cou}(r)$  with a diffraction correction based on the thermal de Broglie length and a Pauli exclusion potential if the spins are parallel. The interaction between two ions is also a Coulomb potential. At astrophysical compressions, the mean proton-proton separation may be small enough to need a treatment where the protons

too are considered as quantum particles. This poses no additional difficulty in CHNC.

The  $B_{ij}(r)$  is the ‘‘bridge’’ term due to certain cluster interactions. If this is neglected, Eqs. 33- 34 form a closed set defining the HNC approximation. The HNC is sufficient for the uniform 3-D electron liquid for a range of  $r_s$ , up to  $r_s = 50$ , as shown previously [48]. Hence we neglect the e-e bridge corrections in this study.

The construction of  $\beta_{eA}, \phi_{eA}(r)$  requires attention. In modeling  $\phi_{eA}(r)$  and  $T_{eA}$  Bredow et al [52] examined the applicability of a very simple electron-ion interaction and a simple model for the inter-subsystem temperature of the two-temperature system.

$$\phi_{eA}^0(r) = -\bar{Z}/r, T_{eA} = (T_{ee}T_{AA})^{1/2}. \quad (35)$$

The existence of a bound core can easily be included by using the form  $\phi_{eA}(r) = \phi_{eS}^0\{1 - \exp(-r_c/\lambda_{th})\}$ . Such a core correction is possible for most ions except hydrogenic ions (bare nuclei). Results improve if a diffraction corrected pseudopotential is used even for hydrogenics.

Thus a more sophisticated approach was used in Ref. [34] where the electron-deuterium pseudopotential was constructed from the NPA model for an ion immersed in the appropriate UEL, when better agreement with quantum simulations can be obtained. That is, if the free-electron density increment around the ion calculated from the NPA is  $\Delta n_{npa}(r)$ , then

$$g_{ei}(r) = \Delta n(r)/\bar{n} \quad (36)$$

$$\beta_{ei}U_{ei}(r) = \text{hnc inversion of: } g_{ei}(r) \quad (37)$$

That is, the quantum mechanical charge density obtained from the NPA (see Fig. 3), when interpreted as a CHNC density already contains the needed electron-ion interaction scaled by an appropriate inverse temperature. The assumption of a simple pseudopotential, which was investigated by Bredow *et al.* is in fact not necessary if the NPA code is invoked.

However, even the simple point-ion model yielded quite good results for the  $H^+ - H^+$  PDFs for warm dense hydrogen where the calculations take only an imperceptible amount of time and even a small laptop can be used. In fig. 4 we display the CHNC results from the simple model of Bredow et al. for warm dense hydrogen [52], and compare with the QMC simulations of Liberatore et al. [53]. At the density used, the neglected ion-ion Bridge correction is probably important, and protons are not strictly classical particles. The QMC simulation treats only the electrons as quantum particles. It is clear from Figs 3,4 that the  $g_{ei}(r)$  obtained from the point-ion model, and using the ansatz  $T_{ei} = \sqrt{T_e T_i}$  is not very satisfactory.

Better agreement is obtained when the simple heuristic models used in Eq. 35 are improved by using NPA densities to construct the needed interaction potentials, as was done for the construction of the Pauli exclusion potential by HNC inversion, eq. 37. Even as it is, the

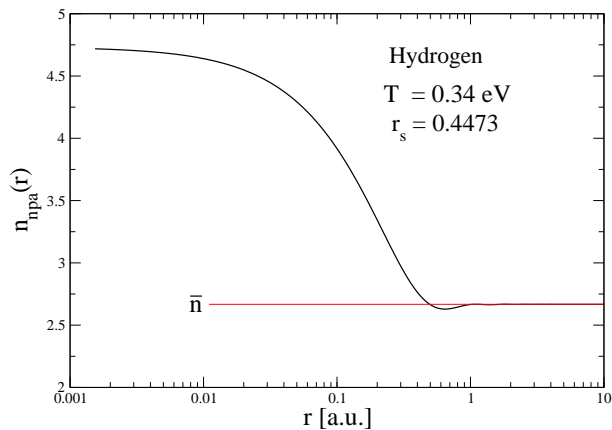


FIG. 3. The free-electron density  $n_{\text{npa}}(r)$  calculated from the NPA model at a proton in a hydrogen plasma,  $T = 0.34$  eV, with an ion density of  $\bar{\rho} = 1.8 \times 10^{25} \text{ cm}^{-3}$ . The excess density  $\Delta n_{\text{npa}}(r) = n_{\text{npa}}(r) - \bar{n}$ , where  $\bar{n} = \bar{\rho} = 2.6473$  electrons or protons per a.u. of volume, can be used to construct the classical pseudopotential  $\beta_{ei}U_{ei}(r)$ , via Eq. 37

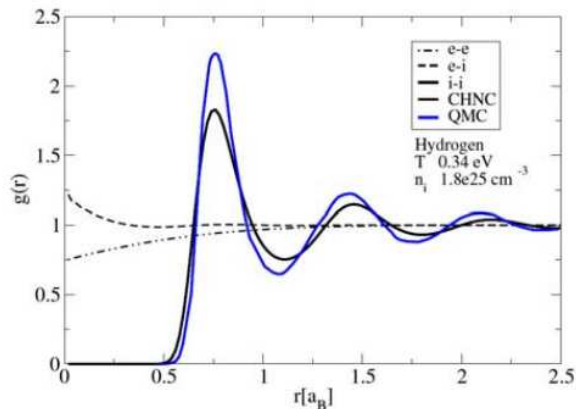


FIG. 4. Pair distribution functions for a fully ionized hydrogen plasma at  $T = 0.34$  eV and an ion density of  $\bar{\rho} = 1.8 \times 10^{25} \text{ cm}^{-3}$  (i.e.,  $\sim 350$  times the density of solid hydrogen). Results of CHNC (black) and QMC (blue) calculations are shown. There is good agreement for peak positions while significant differences in the peak heights exist, showing that the point-ion model and the choice of  $T_{eA}$  via Eq. 35 are only moderately successful. An approach that uses the NPA density is needed to define  $\beta_{ei}U_{ei}(r)$ , as in Eq. 37.

PDFs are sufficiently accurate for rapid evaluations of the Equation of State, which is a property insensitive to small differences in the PDFs. If the ions have an inner core of bound electrons and an effective charge of  $\bar{Z}$ , e.g., for  $\text{Al}^{3+}$ , then the electron-ion interaction must be treated using a pseudopotential with a finite-core radius instead of using the point ion model  $\bar{Z}/r$ , Eq. 35. As the CHNC method cannot as yet yield bound states, it is best to use the two-component NPA model for complex systems, unless one wishes to extract a  $g_{ee}(r)$  for the sys-

tem of electrons in the presence of ions. In all cases, using the NPA  $n_{ei}$  to construct  $\beta_{ei}U_{ei}(r)$  by Eq. 37 should be explored.

The  $N$ -representability of the electron-electron  $g_{ee}(r)$  obtained from the CHNC method needs to be examined. This too can be approached as in the previous section. It appears that  $N$ -representability is preserved in this case too, where we have merely made the electrons to interact with the ‘external potential’ of the ions which is, however, self-consistently adjusted in the two component problem, with no invoking of the Born-Oppenheimer approximation. The BO corrections come through the ion-electron correlation potentials (HNC-like diagrams) contained in the HNC equation describing the  $g_{eA}(r)$  pair distribution function [54].

We may also add that the  $v$ -representability of the densities generated by CHNC, or via the NPA can be treated rather easily since we are dealing entirely with Coulombic systems and spherical charge densities. For such systems, Kato’s theorem [55] applies, and the methods based on spherical densities can be used [56, 57].

## CONCLUSION

A review of the classical map hyper-netted chain procedure, which is a way of side stepping the construction of a quantum kinetic energy functional for density functional theory is presented. A proof of the  $N$ -representability of the classical map, and some plausibility arguments for  $N$ -representability are given. The application of the CHNC method to general electron-ion systems is reviewed where in technically demanding quantum systems like warm dense matter are shown to be affordable, within certain limits, using entirely classical calculations which are very rapid and scale as the zeroth power of the number of particles.

The author thanks Professors Sam Trickey and Jim Dufty for raising the question of the  $N$ -representability of the CHNC procedure at the CECAM workshop at Lausanne, Switzerland, May, 2019.

\* Email address: chandre.dharma-wardana@nrc-cnrc.gc.ca

- [1] A. J. Coleman, Rev. Mod. Phys. **35**, 668 (1963).
- [2] R. Erdahl and V. H. Smith Jr., Eds., *Density Matrices and Density Functionals: Proceedings of the A. John Coleman Symposium* (Reidel, Boston, 1987).
- [3] P. Hohenberg and W. Kohn. Phys. Rev., **136**, B864 (1964)
- [4] L.J. Sham and W. Kohn, Phys. Rev. (1965)
- [5] R. M. Dreizler and E. K. U. Gross, Density Functional Theory, (Springer, Berlin, 1990).
- [6] F. Perrot and M. W. C. Dharma-wardana, Phys. Rev. A **30**, 2619 (1984)
- [7] N. D. Mermin, Phys. Rev. B **1**, 2362 (1970)

- [8] J. E. Mayer, Phys. Rev. 1579 (1955).
- [9] M. Levy, Phys. Rev. A, **26**, 1200, (1982).
- [10] D. A. Mazziott, Phys. Rev. Lett. **108**, 263002 (2012)
- [11] Y. A. Wang and E. A. Carter, Chapter 5 of *Theoretical Methods in Condensed Phase Chemistry*, in book series of *Progress in Theoretical Chemistry and Physics*, edited by S. D. Schwartz, pp. 117-184 (Kluwer, Dordrecht, 2000).
- [12] V. Karasiev, T. Sjostrom, and S. B. Trickey, Phys. Rev. B **86**, 115101 (2012)
- [13] T. G. White, S. Richardson, B. J. B. Crowley, L. K. Pattison, J. W. O. Harris, and G. Gregori, Phys. Rev. Lett. **111**, 175002 (2013).
- [14] Jouko Lehtomäki, Ilja Makkonen, Miguel A. Caro, Ari Harju, and Olga Lopez-Acevedo, J. Chem. Phys. **141**, 234102 (2014) [<http://dx.doi.org/10.1063/1.4903450>].
- [15] J. Clérouin Grégory Robert, Philippe Arnault, Christopher Tricknor, Joel D. Kress, and Lee A. Colins Phys. Rev. E **91** 011101(R), (2015).
- [16] M. W. C. Dharma-wardana and F. Perrot, Phys. Rev. A **26**, 2096 (1982)
- [17] E. K. U. Gross, and R. M. Dreizler, *Density Functional Theory*, NATO ASI series, **337**, p 625, Plenum Press, New York (1993).
- [18] F. Perrot and M.W.C. Dharma-wardana, Phys. Rev. E. **52**, 5352 (1995).
- [19] J. Chihara, Progress in Theoretical Physics **72**, 940 (1984)
- [20] J. A. Anta and A. A. Louis, Phys. Rev. B **61**, 11400 (2000)
- [21] M. W. C. Dharma-wardana and F. Perrot, Phys. Rev. Lett., **65**, 76 (1990).
- [22] M. W. C. Dharma-wardana, Contrib. Plasma Phys. **58** 128-142 (2018)
- [23] G. Kresse and J. Furthmüller, Phys. Rev. B **54**, 11169 (1996).
- [24] X.Gonze and C. Lee, Computer Phys. Commun. **180**, 2582-2615 (2009).
- [25] M. Levy and H. Ou-Yang, Phys. Rev. A **38**, 625 (1988).
- [26] V. Karasiev, S. Trickey, and F. Harris, J. Comput. Aided Mater. Des. **13**, 111 (2006).
- [27] C. J. Umrigar and Xavier Gonze, Phys. Rev. A **50**. 3827 (1994)
- [28] M. W. C. Dharma-wardana and F. Perrot, Phys. Rev. Lett. **84**, 959 (2000)
- [29] François Perrot and M. W. C. Dharma-wardana, Phys. Rev. Lett. **87**, 206404 (2001)
- [30] C. Bulutay and B. Tanatar, Phys. Rev. B **65**, 195116 (2002).
- [31] Chieko Totsuji, Takashi Miyake, Kenta Nakanishi, Kenji Tsuruta and Hiroo Totsuji, J. Phys.: Condens. Matter **21** 045502 (2009)
- [32] J. Dufty, and S. Dutta, Phys. Rev. E **87**, 032101 (2013).
- [33] Yu Liu and Jianzhong Wu, J. Chem. Phys **141**, 064115 (2014)
- [34] Dharma-wardana, M. W. C.; and Perrot, F.; Phys. Rev. B **66**, 014110 (2002)
- [35] M. W. C. Dharma-wardana, D. Neilson and F. M. Peeters, Phys. Rev. B **99**, 035303 (2019) <https://arxiv.org/abs/1901.00895>
- [36] G. D. Mahan, *Many particle Physics*, Sec. 5.1, Plenum Publishers, New York (1981)
- [37] G. F. Giuliani et al., *Quantum Theory of the Electron Liquid.*, Appendix 4, Cambridge University Press (2005)
- [38] M. W. C. Dharma-wardana and F. Perrot, Phys. Rev. B **70**, 035308 (2004).
- [39] M. W. C. Dharma-wardana and François Perrot, Europhys. Letters, **63**, 660 (2003).
- [40] M. W. C. Dharma-wardana, Phys. Rev. B **72**, 125339 (2005).
- [41] F. Lado, J. Chem. Phys. **47**, 5369 (1967).
- [42] M. W. C. Dharma-wardana, J. Phys. Conf. Ser. **442**, 012030 (2013).
- [43] H. Minoo, M. M. Gombert, and C. Deutsch, Phys. Rev. A **23**, 924 (1981).
- [44] G. Kelbg, Ann. Phys. **467**, 219 (1963).
- [45] A. V. Filinov, V. O. Golubnychiy, M. Bonitz, W. Ebeling, and J. W. Dufty, Phys. Rev. E **70**, 046411 (2004).
- [46] Singwi, M. P. Tosi, R. H. Land, and A. Sjölander, Phys. Rev. **176**, 589 (1968).
- [47] P. Vashista and K. S. Singwi, Phys. Rev. B **6**, 875 (1972).
- [48] F. Perrot and M. W. C. Dharma-wardana, Phys. Rev. B **62**, 16536 (2000); *Erratum:* **67**, 79901 (2003); arXiv-1602.04734.
- [49] F. Lado, S. M. Foiles and N. W. Ashcroft, Phys. Rev. A **26**, 2374 (1983).
- [50] W. E Brown, J. L. DuBuois, M. Holzmann and D. M. Ceperley, Phys. Rev. B **88**, 081102 (2013).
- [51] V. V. Karasiev, T. Sjostrom, J. W. Dufty, and S. B. Trickey, Phys. Rev. Lett. **112**, 076403 (2014).
- [52] R. Bredow, Th. Bornath, W.-D. Kraeft, M.W.C. Dharma-wardana and R. Redmer Contributions to Plasma Physics, **55**, 222-229 (2015) DOI 10.1002/ctpp.201400080
- [53] E. Liberatore, C. Pierleoni, and D. Ceperley, J. Chem. Phys. **134**, 184505 (2011).
- [54] F. Perrot, Y. Furutani and M.W.C. Dharma-wardana, Phys. Rev. A **41**, 1096-1104 (1990)
- [55] T. Kato, Commun. Pure Appl. Math. **10**, 151 (1957).
- [56] A. Theophilou, J. Chem. Phys. **149**, 074104 (2018)
- [57] J. Chem. Phys. **149**, 204112 (2018)